Science and Technology Indonesia
e-ISSN:2580-4391 *p*-ISSN:2580-4405
Vol. 8, No. 4, October 2023

Research Paper

Extreme Drought Assessment in Sumatra-Indonesia Using SPI and EDI

Suhadi[1], Iskhaq Iskandar[2*], Supari[3], Muhammad Irfan[2], Hamdi Akhsan[1]

[1]*Graduate School of Sciences, Faculty of Mathematics and Natural Sciences, Sriwijaya University, 30862, Indonesia*
[2]*Department of Physics, Faculty of Mathematics and Natural Sciences, Sriwijaya University, 30862, Indonesia*
[3]*Indonesia Agency for Meteorology, Climatology and Geophysics BMKG, Jl.Angkasa I No 2 Kemayoran, Jakarta, 3540, Indonesia*
***Corresponding author**: iskhaq@mipa.unsri.ac.id

Abstract
Even though Sumatra is very vulnerable to the effects of drought, research identifying drought on this island is very limited, especially extreme drought. This research was conducted to identify extreme drought in Sumatra using the Standardized Precipitation Index (SPI) and the Effective Drought Index (EDI). This study uses precipitation data from the Indonesian Meteorology, Climatology and Geophysics Agency (BMKG) and Global Precipitation Climatology Center (GPCC) reanalysis data. The composite indices were conducted to discover some phenomena that cause the drought based on El Niño and positive Indian Ocean Dipole (IOD) events. The results showed that the El Niño and positive IOD phenomena were more likely to influence extreme droughts. However, the droughts in 2014 and 2008 tended to be influenced by the negative Sea Surface Temperature anomaly (SSTA). The spatial analysis results show that the areas that experience extreme drought more often are the west coast of Sumatra (except Aceh province), especially based on SPI12 and EDI. The composite indices results show that the drought that occurred in Aceh province was more influenced by the El Niño phenomenon in the December-January-February (DJF) period and the positive IOD in the June-July-August (JJA) – September-October-November (SON) period. In addition, Aceh province is an area that is not affected by El Niño-positive IOD, especially during the SON-DJF period. These results can be used to mitigate drought, especially when El Niño-positive IOD phenomena cause it.

Keywords
Extreme Drought, Sumatra, Indonesia, Standardized Precipitation Index, Effective Drought Index, El Niño, Positive IOD

Received: 11 May 2023, Accepted: 5 September 2023
https://doi.org/10.26554/sti.2023.8.4.691-700

1. INTRODUCTION

As an annual natural disaster that impacts various sectors of life (WMO, 2016), drought is a condition with lower precipitation than usual in certain areas and periods (WMO, 2012). Referring to the impact of drought, the four types of drought defined by the World Meteorological Organization (WMO) are Meteorological Drought, Agricultural Drought, Hydrological Drought, and Socio-Economic Drought (Svoboda and Fuchs, 2016; WMO, 2016). The four droughts usually occur sequentially, depending on how long the drought lasts. Meteorological drought is influenced by precipitation as the main indicator (Abbas et al., 2021; Bougara et al., 2021; Eslamian et al., 2017; Salehnia et al., 2017) is the drought that occurs in the first stage. This drought then continues as an agricultural drought (Adisa et al., 2021), marked by reduced soil moisture and causing damage to agriculture. The third stage of this drought is a hydrological drought marked by the diminishing water supply in the river. The third stage of this drought is hydrological drought, marked by the diminishing supply of water in the river (Eslamian et al., 2017; Zargar et al., 2011). In the end, this drought will impact the socio-economic sector. Not only in the socio-economic sector but in some serious cases, such as in Africa, the impact of this drought has resulted in death (Adisa et al., 2021). One of the efforts that can be made to mitigate the impact of the drought is a drought assessment.

In conducting a drought assessment, there are at least 23 meteorological drought indices with difficulty levels of use, namely easy, medium, and difficult (Svoboda and Fuchs, 2016; WMO, 2016). The ease of use of these various indices is usually determined based on the input parameters used. Apart from this level of convenience, of course, this use is due to the advantages and disadvantages of the indices, which usually refer to the topographical conditions of an area (Adisa et al., 2021). Several studies have been conducted to analyze a suitable index for assessing a drought that has occurred. For example, the Percent Normal Index (PN) and Rainfall Anomaly Index (RAI) detect more droughts occurring in the Tafna-Northwestern Algeria watershed than the Standardized Precipitation Index

(SPI) and Decile Index (DI). Bougara et al. (2021) show that PN and RAI detect more than droughts detected by SPI. Meanwhile, EDI is more sensitive than SPI in detecting drought in Bangladesh (Kamruzzaman et al., 2019). However, SPI is an index the WMO recommends to detect drought (Svoboda and Fuchs, 2016; WMO, 2016).

Apart from being recommended by the WMO, SPI is a widely used method (Chandrasekara et al., 2021), which McKee et al. (1993) introduced to detect meteorological drought in Colorado. However, this index is weak because it only uses precipitation to indicate drought. Another method that uses precipitation as calculation input is EDI. Byun and Wilhite (1999) introduced EDI to overcome the lack of SPI. EDI uses a precipitation time reduction function, claimed as an evapotranspiration calculation not used in SPI calculations. As a new method, EDI has been used by several researchers in detecting drought. In South Africa, EDI (and SPI) have been used to detect drought (Adeola et al., 2021; Adisa et al., 2021). In a recent study, the EDI was modified to determine the impact of social drought on the Korean Peninsula (Park et al., 2022).

Sumatra is a region often affected by drought, especially in the environmental sector (Davies and Unam, 1999; Nurdiati et al., 2021; Prinz, 2009; Sarmiasih and Pratama, 2019) in the form of forest and land fires. Even Supari et al. (2016) show that Sumatra is drought-prone, especially in July-October. In 1997/98, several areas of Sumatra (namely, South Sumatra, Riau, and Jambi) experienced drought-related forest fires (Prinz, 2009). This fire then causes an effect in the form of an increase in air pollutants such as SO_2, CO, CH_4 and CO_2 (Davies and Unam, 1999). Apart from 1997/98, the impact of a more severe drought occurred in 2015/16. The drought that happened that year caused forest fires covering an area of 2.6 million ha and was a wider fire than the fires in 2019, which caused forest fires covering an area of 328,722 ha (Sarmiasih and Pratama, 2019). The extent of this burned area is also indicated based on the increase in hotspots in South Sumatra (Nurdiati et al., 2021). Even though the impact of this drought is very significant, research related to drought, especially the extreme drought in Sumatra, is still limited. Therefore, carrying out a drought assessment as a disaster mitigation effort is necessary. So far, most of the drought identification has been carried out in the central to eastern parts of Indonesia (Kuswanto et al., 2019; Nurdiati et al., 2021; Pramudya et al., 2019), particularly in Java and Kalimantan. Therefore, this research used the SPI and EDI methods to identify drought, especially extreme drought in Sumatra.

2. EXPERIMENTAL SECTION

2.1 Location

The research area is Sumatra, as shown in Figure 1. In the western part of Indonesia, this island is an area with precipitation variability triggered by the Asia-Australia monsoon (Iskandar et al., 2011). Apart from Monsoon, ENSO - IOD is also a phenomenon that affects the precipitation on this island during

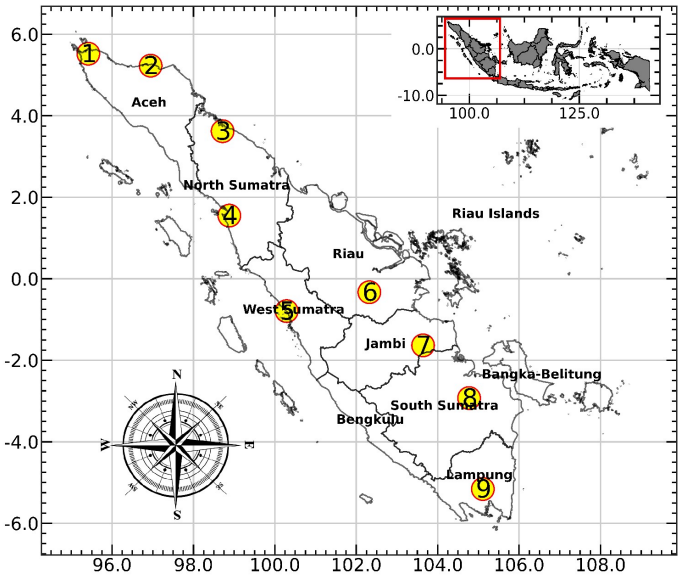

Figure 1. The Area of Interest of Research. The Numbers Indicated in Yellow are Rainfall Stations

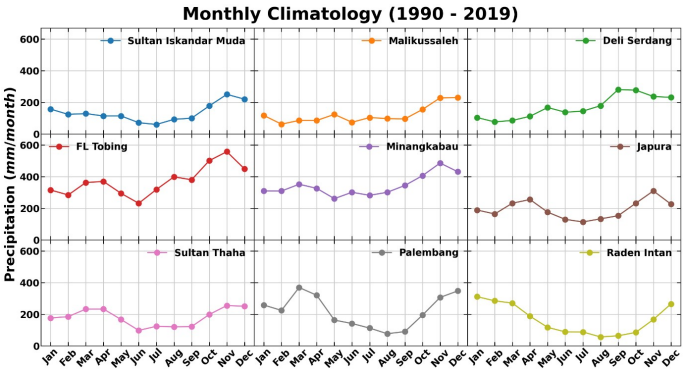

Figure 2. Monthly Climatology in 9 Rainfall Station

interannual periods (Aldrian and Dwi Susanto, 2003; Avia and Sofiati, 2018; Saji and Yamagata, 2003; Iskandar et al., 2017a; Supari et al., 2016). In addition to the precipitation variability, several unique precipitation patterns occur on this island, especially in the northern region (Darlan et al., 2020). This uniqueness changes the opposite pattern from other regions; when the Southern region enters the wet season, this part experiences drought and vice versa (Iskandar et al., 2017b). In contrast, this uniqueness occurs in the SON period of El Niño (Qian, 2020). Topographically, contrasting elevation differences along the western and eastern coasts are also visible on this island. In the part of the west of the island lies the Bukit Barisan, which stretches from north to south. While in the east, there are many rivers and swamps.

2.2 Materials

In this study, we used precipitation station data from the BMKG website, namely http://dataonline.bmkg.go.id. At this site, 33

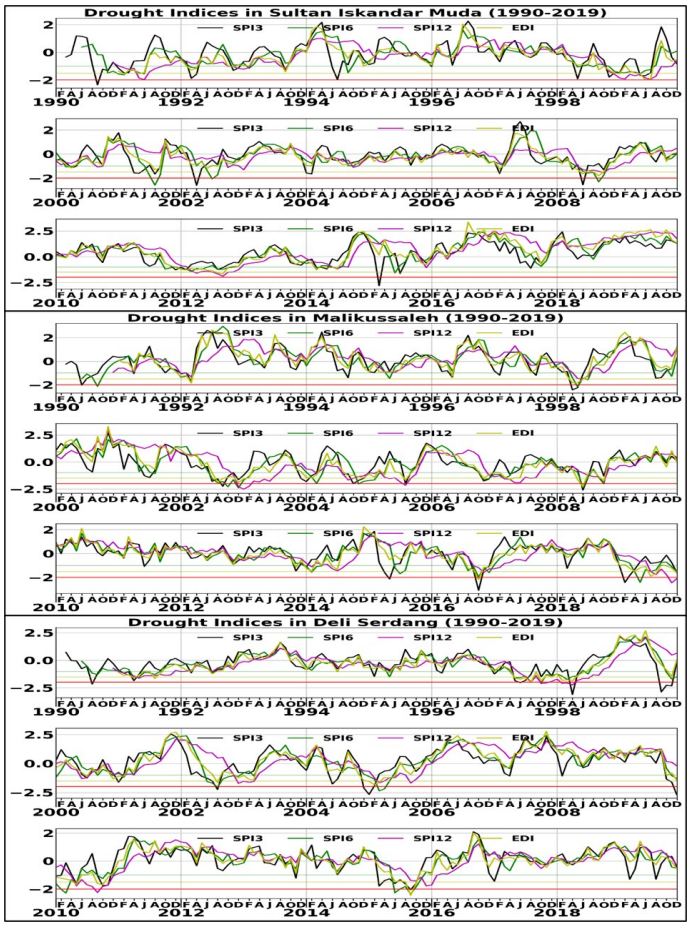

Figure 3. Drought Indices in the Sultan Iskandar Muda, Malikussaleh, and Deli Serdang Rain Gauges. The Horizontal Green, Yellow, and Red Lines are Moderate, Severe, and Extreme Drought Limits

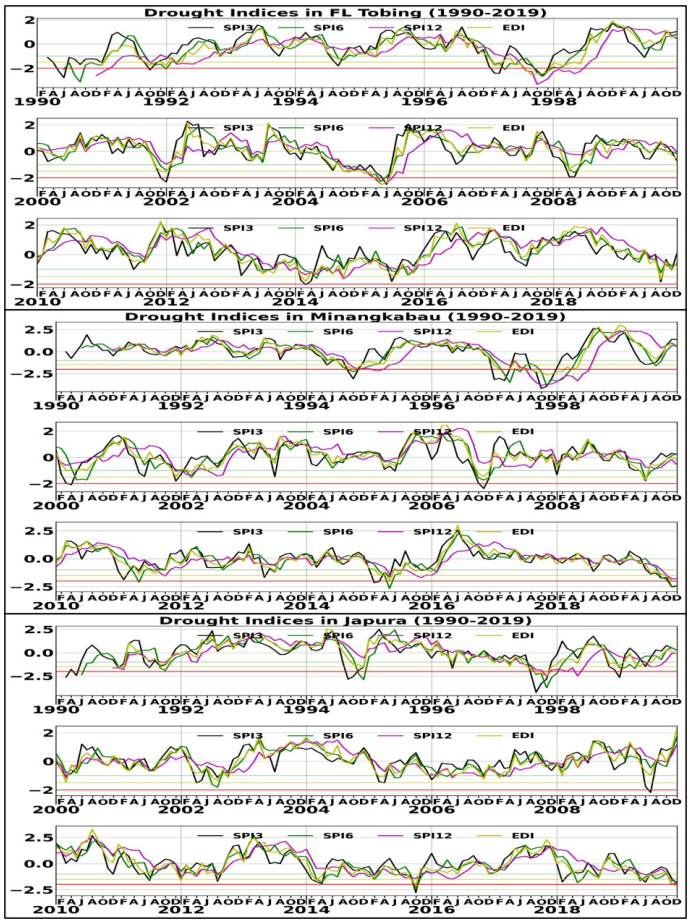

Figure 4. Same with Figure 2, but for the FL Tobing, Minangkabau, and Japura Rain Gauges

rainfall stations spread along Sumatra. However, due to the availability of data at each station and the need for data for at least 30 years, this study only used nine stations, as shown in Table 1. The period of this data is from January 1990 to December 2019. Precipitation data from these BMKG stations will be used to identify extreme drought time series in Sumatra from January 1990 to December 2019.

In addition to using BMKG precipitation data, this research uses Global Precipitation Climatology Center (GPCC) reanalysis data. This reanalysis data has various resolutions, namely 0.25°, 0.5°, 1° and 2.5°. However, this study uses data with a resolution of 0.25° from January 1990 to December 2019. This reanalysis data will be used to see the frequency distribution of extreme droughts over 30 years.

2.3 Methods

2.3.1 SPI

SPI is a method that determines precipitation conditions based on the gamma distribution function (Edwards and McKee, 1997; McKee et al., 1993). Calculation of precipitation conditions is done through several steps. The first step in calculating the SPI is to fit the precipitation data (at least 30 years) to the cumulative gamma distribution function (Adisa et al., 2021; Huang et al., 2016).

$$G(P_j) = \frac{1}{\beta^{\alpha}\Gamma(\alpha)} \int_0^{p_j} P_j^{\alpha-1} e^{-P_j/\beta} dP_j \quad (1)$$

where α and β are the form factor and scale factor respectively, P_j is the accumulated precipitation for j-month, and the gamma function is marked with $\Gamma(\alpha)$. One characteristic of the gamma function is that it cannot be calculated when P_j=0. To overcome this, the cumulative distribution function $G(P_j)$ is changed to

$$H(p_j) = q + (1-q)G(P_j) \quad (2)$$

where q is the probability of zero precipitation, after the cumulative distribution function H(s) is standardized, the final step is to convert this cumulative distribution function into an SPI value using the following approximation technique (Abramowitz and Stegun, 1964).

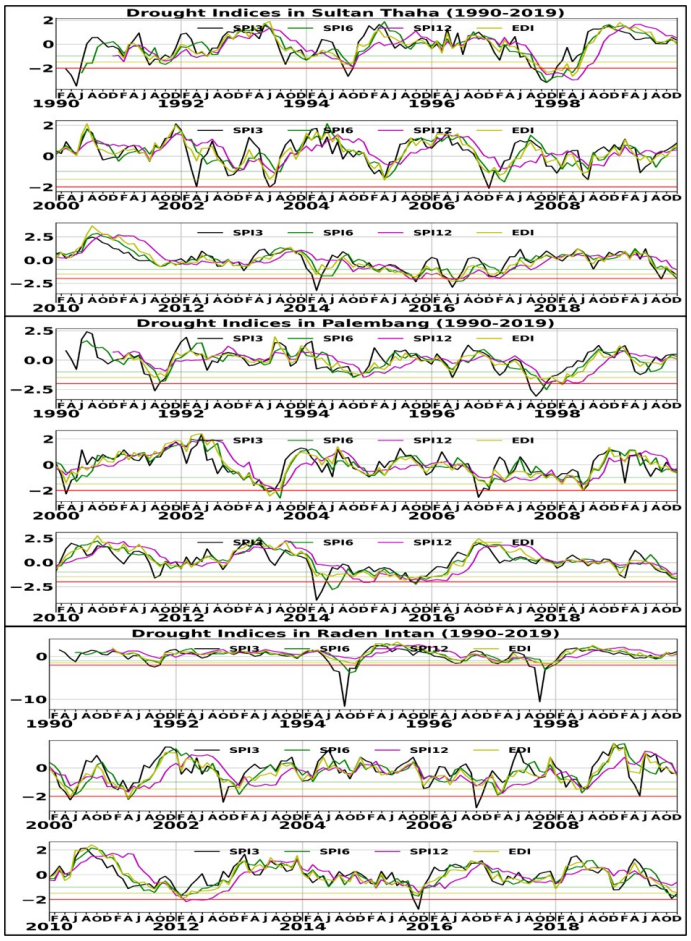

Figure 5. Same with Figure 2, but for the Sultan Thaha, Palembang, and Raden Intan Rain Gauges

$$SPI = -\left(t - \frac{c_0 + c_1 t + c_2 t^2}{1 + d_1 t + d_2 t^2 + d_3 t^3}\right);$$
$$t = \sqrt{ln\left(\frac{1}{H(P_j)^2}\right)} \text{ for } 0 < H(P_j) < 0.5 \quad (3)$$

$$SPI = +\left(t - \frac{c_0 + c_1 t + c_2 t^2}{1 + d_1 t + d_2 t^2 + d_3 t^3}\right);$$
$$t = \sqrt{ln\left(\frac{1}{(1 - H(P_j))^2}\right)} \text{ for } 0.5 < H(P_j) < 1 \quad (4)$$

with c_0 = 2.515517, c_1 = 0.802853, c_2 = 0.010328, d_1 = 1.432788, d_2 = 0.189269, d_3 = 0.001308. SPI can be calculated using accumulated precipitation at various time scales, namely 1, 3, 6, 9, 12, and 24 months. However, in this study, the accumulated precipitation used is 3, 6, and 12 months to analyze drought on a 3-month, 6-month, and 12-month scale.

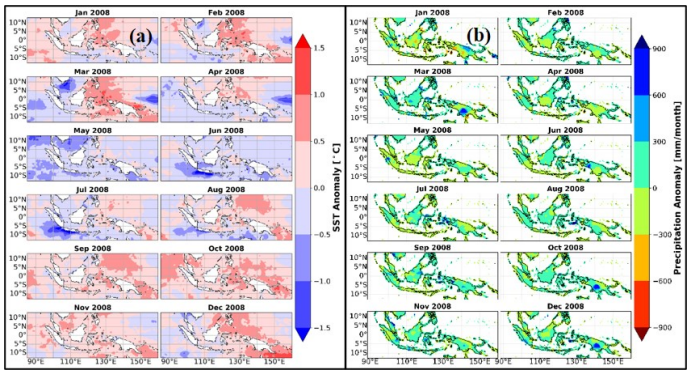

Figure 6. (a) Sea Surface Temperature, and (b) Precipitation Anomaly in 2008

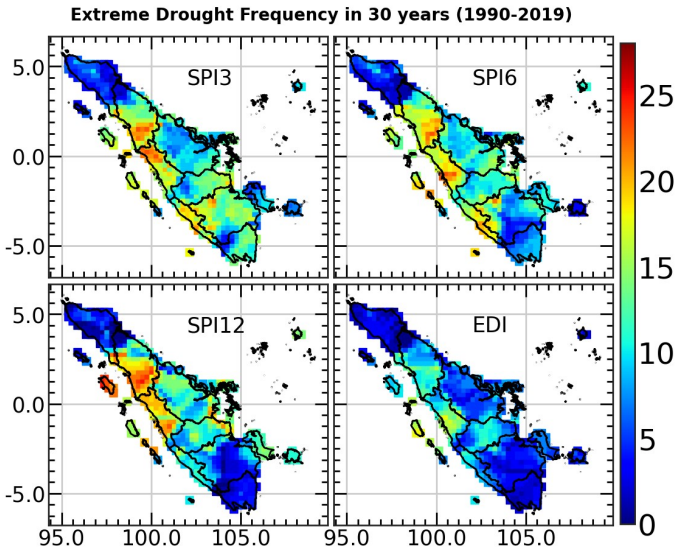

Figure 7. Extreme Drought Frequency of SPI3, SPI6, SPI12, and EDI

2.4 EDI

EDI was introduced by Byun and Wilhite (1999) to identify precipitation conditions based on effective precipitation (EP).

$$EP_i = \sum_{m=1}^{N} \left[\left(\sum_{j=1}^{m} P_j\right)/j\right] \quad (5)$$

The EDI value is calculated based on the ratio between the precipitation needed to return to normal (Precipitation Return to Normal - PRN) and its standard deviation.

$$EDI_i = \frac{PRN_i}{\sigma(PRN_i)} \quad (6)$$

σ (PRN_i) is the standard deviation of PRN in each calendar month (standard deviation of PRN climatology). PRN is calculated based on Jain et al., 2015; Raude et al., 2018.

Table 1. Rainfall Stations

Rainfall Stations	Lat	Lon
Sultan Iskandar Muda	5.52	95.42
Malikussaleh	5.23	96.95
Deli Serdang	3.62	98.71
FL Tobing	1.55	98.88
Minangkabau	-0.79	100.29
Japura	-0.33	102.32
Sultan Thaha	-1.63	103.64
Palembang	-2.98	104.77
Raden Inten	-5.16	105.11

$$PRN_i = DEP_i / \left(\sum_{j=1}^{N} \frac{1}{j} \right) \quad (7)$$

$$DEP_i = EP_i - \bar{EP}_l \quad (8)$$

DEP and $\bar{EP}_l$ are the deviation of the effective precipitation and the average precipitation in each calendar month (climatological average), respectively. Precipitation conditions (dry or wet) identified using SPI and EDI are determined based on the scale shown in Table 2.

Table 2. SPI and EDI Scales

Conditions	SPI/EDI
Extremely Drought	≦ -2.00
Severely Drought	-1.5 to -1.99
Moderately Drought	-1.0 to -1.49
Normal	-0.99 to 0.99
Moderately Wet	1.0 to 1.49
Severely Wet	1.5 to 1.99
Extremely Wet	≧ 2.00

As is known, several factors related to drought are El Niño and positive IOD. To find out the relationship between this phenomenon and the drought, we used the period of El Niño positive and IOD from 1990 to 2020. We obtained data for positive IOD and El Niño by calculating the Sea Surface Temperature (SST) in the IOD and Niño3.4 blocks. This SST data is ERA5 reanalysis data with a resolution of 0.25°. After calculating, the positive IOD and El Niño events obtained are shown in Table 3. El Niño and positive IOD conditions are determined based on the Standard Deviation of Sea Surface Temperature Anomaly (SSTA). We then use the period (season) that shows positive El Niño and IOD events as the basis for composite calculations of SPI3, SPI6, SPI12, and EDI. We only include months showing El Niño and positive IOD phenomena in one season to ensure accurate composite results. For example, El Niño in 2009 in SON started in October-November, so the composite index (SPI3, SPI6, SPI12, and EDI) was only carried out in October-November.

3. RESULTS AND DISCUSSION

3.1 Precipitation Climatology

The monthly precipitation climatology of the nine stations is shown in Figure 2. These results indicate that in the period from January to August (JFMAMJJA), precipitation at the Sultan Iskandar Muda, Malikukksasaleh and Deli Serdang stations was less than 200 mm. This condition is also shown by Qian (2020), which states that the northern region of Sumatra tends to experience precipitation of more than 200mm during the SON period. Apart from being due to the west monsoon winds, which bring a mass of water from Asia to Australia, this is also due to the more dominant westerly winds that blow from the Indian Ocean Qian (2020). Monthly precipitation recorded at 200mm/month-550mm/month at FL Tobing and Minangkabau stations indicates that these two stations experience higher precipitation than the other seven stations. This higher precipitation is because the Tobing and Minangkabau FL station areas directly face the Indian Ocean, so the IOD phenomenon affects this region (Iskandar et al., 2011; Lee, 2015; Mori et al., 2004). The highest precipitation at this station occurs in November, and another peak in March. Precipitation patterns at Japura, Sultan Thaha, and Palembang stations are the same as the previous stations (FL Tobing and Minangkabau). These three stations' precipitation patterns also show peaks in March and November.

Nonetheless, the precipitation is lower than at the FL Tobing and Minangkabau stations. This condition is due to the obstruction of the mass of seawater (brought by the westerly wind) by the Bukit Barisan, which stretches along the western side of Sumatra. Unlike the others, the peak of precipitation at the Raden Intan station occurs in January (DJF season). As previously explained, this condition was also shown by Qian (2020) that the northern part of Sumatra tends to experience higher precipitation at SON while the southern region at DJF. If sorted by the amount of monthly precipitation, it can be seen that the high precipitation respectively is TM (FL Tobing-Minangkabau), JSPR (Japura-Sultan Thaha-Palembang-Raden Intan), and IMD (Sultan Iskandar Muda-Malikussaleh-Deli Serdang).

3.2 Temporal Analysis

The results of drought identification based on SPI3, SPI6, SPI12, and EDI are temporally shown in Figure 3-5. Figure 3 for Sultan Iskandar Muda, Malikussaleh and Deli Serdang stations, Figure 4 for FL Tobing, Minangkabau and Japura stations, and Figure 5 for Sultan Thaha, Palembang and Raden Intan stations. As it is known that, generally, the drought that occurs, especially in Indonesia, is caused by a positive El Niño - IOD. For example, the droughts of 1997/98 and 2015/16. The El Niño - positive IOD that occurs simultaneously causes these droughts. In 1997/98, the drought reached

Table 3. El Niño and Positive IOD Event. (A) for August, (ON) for Oct and November, (MA) for March and April, (M) for March, (..M) for May, (JA) for July and August, (SO) for September and October, (D) for December, and (J) for January

Phenomena	Periods	Years
El Niño	JJA	2002(A)
	SON	1991(ON); 2002; 2009(ON)
	DJF	1991/92; 2002/03(J); 2009/10
	MAM	1992(MA); 2010(M)
Positive IOD	JJA	2011(A); 2012(JA); 2019
	SON	2011(SO); 2012(SO); 2019
El Niño and	JJA	1994(JA); 1997; 2006(A); 2015
Positive IOD	SON	1994; 1997; 2006; 2015
	DJF	1994/95(J); 1997/98; 2006(D); 2015/16
	MAM	1998(MA); 2015(..M); 2016(MA)

extreme levels at Malikussaleh stations (SPI3, SPI6), Deli Serdang (SPI3, SPI6, SPI12), FL Tobing (SPI3, SPI6, SPI12, EDI), Minangkabau (SPI3, SPI6, SPI12, EDI), Japura (SPI3, SPI6, SPI12, EDI), Sultan Thaha (SPI3, SPI6, SPI12, EDI), Palembang (SPI3, SPI6, SPI12, EDI), Raden Intan (SPI3, SPI6, SPI12, EDI). Whereas in 2015/16, extreme drought was detected at Sultan Iskandar Muda (SPI3), Malikussaleh (SPI3), Deli Serdang (SPI6, EDI), Minangkabau (SPI3, SPI6), Japura (SPI3, SPI6, EDI), Sultan Thaha (SPI3, SPI6, SPI12, EDI), Palembang (SPI3, SPI6), and Raden Intan (SPI3). El Niño in 2009/10 caused extreme drought to be detected at Deli Serdang station (SPI6, SPI12), Japura (SPI3). Whereas the positive IOD in 2012 caused extreme drought, only detected at the Raden Intan station (SPI3). In addition to the extreme drought caused by the positive El Niño-positive IOD phenomena, several droughts unrelated to these phenomena also occurred in 2008 at the Sultan Iskandar Muda station (SPI3, SPI6), Malikussaleh (SPI6, EDI). In addition to the extreme drought in 2008, the 2014 drought was not caused by the El Niño-positive IOD phenomena but by the negative SSTA (Iskandar et al., 2017a).

In Figure 6a, it can be seen that a strong negative sea surface temperature anomaly occurred in the May-June-July period. This anomaly caused a reduction in the mass convection activity of seawater into the atmosphere in that period (Figure 6b), which in turn led to reduced precipitation, especially on the island of Sumatra. This negative SSTA was also the cause of the drought that occurred on the island of Java in 2008 (Nita et al., 2020).

3.3 Spatial Analysis

The results of identifying extreme droughts are spatially shown based on the frequency of extreme droughts, as shown in Figure 7. This frequency indicates the number of extreme droughts that have occurred in 30 years (1990-2019). Based on SPI3 calculations which describe precipitation conditions for three months, extreme droughts ranging from 10-22 times occurred almost along the west coast of Sumatra, more precisely in the south of North Sumatra, West Sumatra, Bengkulu, and most

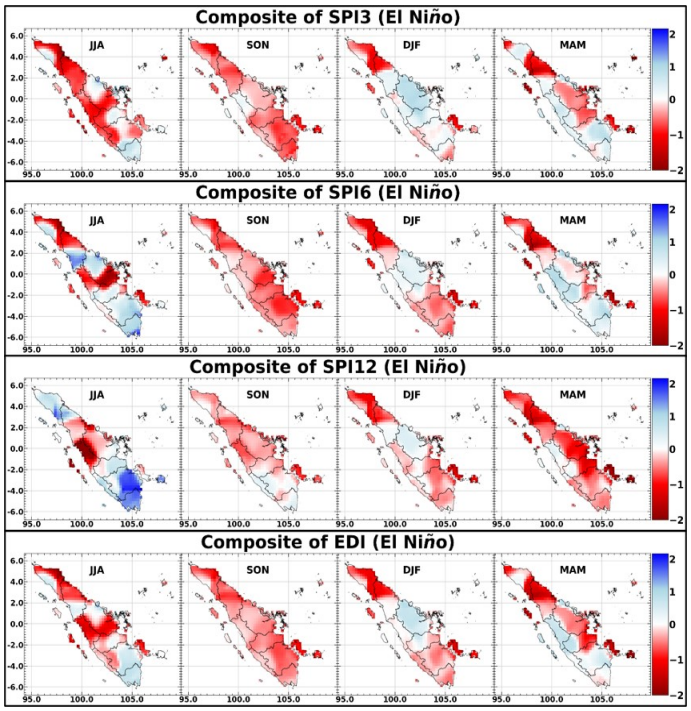

Figure 8. Composite of Indices in El Niño Events

of South Sumatra.

Drought analysis based on SPI6 shows that the frequency of extreme droughts is as much as 10-25 times more visible in the provinces of North Sumatra, West Sumatra, Bengkulu, to a small part of South Sumatra. Most of the drought frequency in this region has been detected based on SPI3, except for the east coast of South Sumatra and Lampung, which were detected to show a decrease in the frequency of extreme drought. SPI12 detects the number of extreme droughts around 20-25 times occurring in the southern provinces of North Sumatra and West Sumatra. The frequency distribution of extreme droughts shown by EDI is the same as that shown by SPI12, and it is just that the number of extreme droughts detected by EDI is

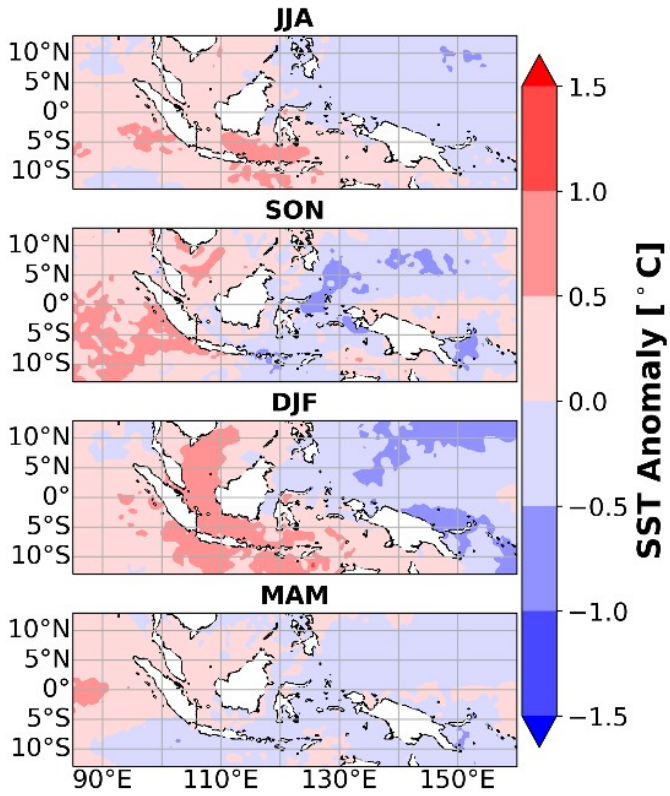

Figure 9. Sea Surface Temperature Anomaly in El Niño

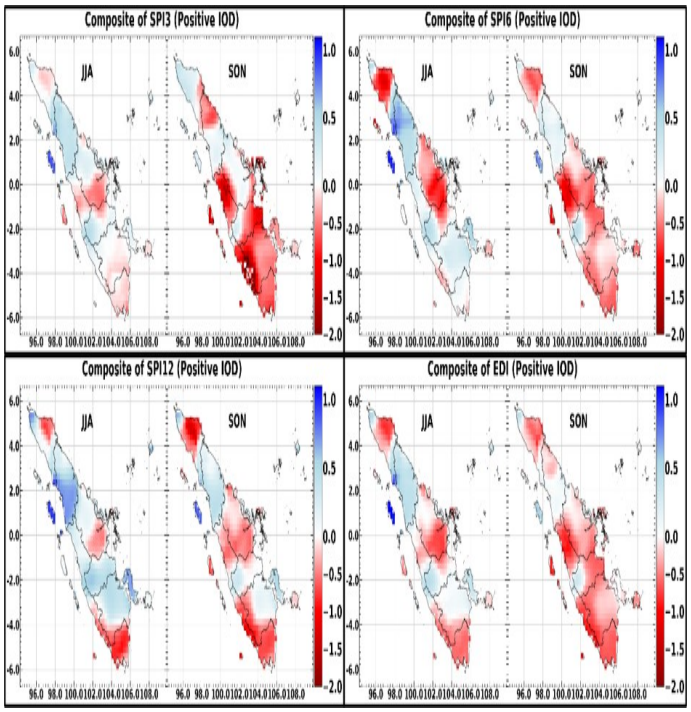

Figure 10. Composite of Indices in Positive IOD Events

less than SPI12. EDI detects the number of extreme droughts in the south of North Sumatra province about ten times and in West Sumatra about 17 times. The lowest extreme drought frequency detected by EDI occurred in Aceh Province. It was also shown by Supari et al. (2023).

As previously explained, SPI3, SPI6, SPI12, and EDI describe precipitation conditions (dry/wet) on a 3-month, 6-month, and 12-month scale. Based on the frequency of extreme droughts, it can be seen that the distribution of extreme droughts on a seasonal scale is wider than on inter-seasonal and annual scales. The areas that often experience drought (3-month, 6-month, and 12-month scale) are West Sumatra to the southern part of North Sumatra. This condition is related to research by Daoed et al. (2018), which shows that West Sumatra tends to be vulnerable to drought, especially in river basins. The climatological results in section 3.2 show that this area (Tobing and Minangkabau FL stations) has the highest monthly precipitation. However, this area has tended to experience more extreme drought over the past 30 years. This result shows that identifying drought with SPI and EDI is local, which refers to regional precipitation. Regions with low precipitation throughout the year do not always refer to drought because drought refers to the condition of below-normal precipitation in a certain area and time. In addition, these results also show that SPI and EDI, in particular, cannot detect drought spatially.

3.4 Drought Correlation with El Niño and Positive IOD

The composite of SPI3, SPI6, SPI12, and EDI results at the time of El Niño, positive IOD, and El Niño-positive IOD, respectively, are shown in Figure 8, Figure 10, and Figure 11. El Niño is more dominant on SON, mainly based on SPI3, SPI6, and EDI composites. During the JJA period, the influence of El Niño (SPI3 composite) tends to occur in the northern provinces of Aceh, North Sumatra, West Sumatra, and parts of Riau to Bengkulu. In this period (JJA), the SPI12 composite showed a more dominant El Niño effect in the province of West Sumatra. In the DJF period, it can be seen that El Niño is more dominant in the north, while in the MAM period, El Niño is more dominant on the east coast of Sumatra. When El Niño occurs, almost the entire area of Sumatra experiences drought, especially during the SON to MAM seasons. However, dry-normal conditions were exchanged in the provinces of Riau and Bengkulu during the DJF and MAM seasons.

During the DJF season, Riau province tends to be in normal conditions, while Bengkulu province tends to be dry, and vice versa during the MAM season. This normal condition is because, during the DJF season, there is an increase in sea surface temperature, especially on the coast of Riau province (Figure 9). In addition, this DJF period is the beginning of the monsoon cycle, and The dominant Inter-Tropical Convergence Zone (ITCZ) is at the equator Qian (2020). It causes an increase in the convection of water mass activity in the air, and this area experiences an increase in precipitation, so Riau province tends to be in normal conditions. During the MAM season, the sea surface temperature around this area is colder

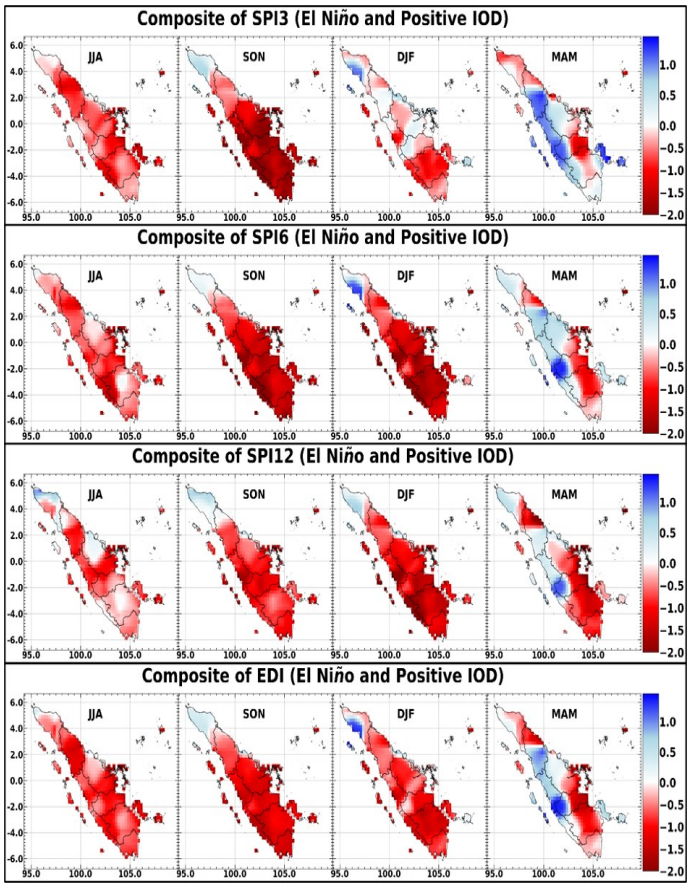

Figure 11. Composite of Indices in El Niño and Positive IOD Events

again, like in the JJA and SON seasons.

The composite drought indices during the positive IOD period are shown in Figure 10. At the beginning of the positive IOD (JJA), the positive IOD influence was more dominant in the provinces of Aceh, West Sumatra-Riau, and Bengkulu-Lampung. The effect of this positive IOD is getting stronger in the SON period. Based on the SPI3 composite, the areas that are dominantly affected by positive IOD are the northern part of North Sumatra, West Sumatra, and parts of Jambi to Lampung provinces. The influence of IOD on the 6-month (SPI6) and 12-month (SPI12 and EDI) scales is more than dominant in the areas of Aceh, Riau, to Lampung.

The effect of El Niño-positive IOD based on the SPI3, SPI6, SPI12, and EDI composites (Figure 11) is the same as when an El Niño occurs. However, when these two phenomena occur simultaneously, the effect of drought is stronger. Based on the SPI3 and SPI6 composites, the influence of these two phenomena is more dominant in the JJA to DJF seasons. Although based on the SPI6 composite, the influence of this phenomenon is slightly weakened in the JJA season, it has strengthened in the MAM season. The influence of these two phenomena was also shown based on the EDI composite. However, during the JJA season, the EDI composite showed the El Niño-positive IOD effect stronger than the SPI6 composite but weaker than the SPI3 composite. The SPI12 composite shows a more dominant El Niño-positive IOD effect in the SON to MAM season.

4. CONCLUSION

Based on the monthly precipitation amount, the west coast of Sumatra receives the highest precipitation throughout the year (TM stations). In contrast, the lowest is on the northern coast of northern Sumatra (IMD stations). In addition, the peak of precipitation in the northern part of Sumatra occurs during the SON period, while the southern part experiences a lack of precipitation. Extreme drought on a 3-month scale tends to be spread across almost all of Sumatra except for Aceh province, which experiences the least extreme drought. The frequency of drought on a 12-month scale is most frequent in the provinces of West Sumatra and southern North Sumatra. In addition, the results of this study indicate that SPI12 detects more extreme drought than EDI. However, the distribution of extreme drought frequencies detected based on EDI is comparable to SPI12. Huang et al. (2016) suggest a strong correlation between SPI12 and EDI. Based on the results of the temporal analysis, it appears that some extreme droughts are not affected by El Niño-positive IOD phenomena, such as the extreme droughts in 2014 and 2008, which negative SSTA more influenced, so some droughts that are not related to these phenomena are thought to be caused by negative SSTA. El Niño is more than dominant in northern Sumatra, especially during the DJF period. Positive IOD is more influential in this region during JJA-SON, as shown in the study by Kurniadi et al. (2021). The southern part of Sumatra is also affected by positive IOD, especially during the SON period. When an El Niño-positive IOD occurs simultaneously, North Sumatra to Lampung is more dominantly affected by this phenomenon, especially during the SON-DJF period. It was also shown by Kurniadi et al. (2021) and Nurdiati et al. (2022).

5. ACKNOWLEDGMENT

This study is part of the first author's dissertation supported by the Ministry of Education, Culture, Research, and Technology through Hibah Penelitian Disertasi Doktor 2022, No. 142/E5/PG.02.00.PT/2022.

REFERENCES

Abbas, A., M. Waseem, W. Ullah, C. Zhao, and J. Zhu (2021). Spatiotemporal Analysis of Meteorological and Hydrological Droughts and their Propagations. *Water*, **13**(16); 2237

Abramowitz, M. and I. A. Stegun (1964). *Handbook of Mathematical Functions with Formulas, Graphs, and Mathematical Tables*, volume 55. US Government Printing Office

Adeola, O. M., M. Masinde, J. O. Botai, A. M. Adeola, and C. M. Botai (2021). An Analysis of Precipitation Extreme Events based on the SPI and Edi Values in the Free State Province, South Africa. *Water*, **13**(21); 3058

Adisa, O. M., M. Masinde, and J. O. Botai (2021). Assessment of the Dissimilarities of EDI and SPI Measures for Drought Determination in South Africa. *Water*, **13**(1); 82

Aldrian, E. and R. Dwi Susanto (2003). Identification of Three Dominant Rainfall Regions within Indonesia and their Relationship to Sea Surface Temperature. *International Journal of Climatology: A Journal of the Royal Meteorological Society*, **23**(12); 1435–1452

Avia, L. and I. Sofiati (2018). Analysis of El Niño and IOD Phenomenon 2015/2016 and Their Impact on Rainfall Variability in Indonesia. *Conference Series: Earth and Environmental Science*, **166**(1); 012034

Bougara, H., K. Baba Hamed, C. Borgemeister, B. Tischbein, and N. Kumar (2021). A Comparative Assessment of Meteorological Drought in the Tafna Basin, Northwestern Algeria. *Journal of Water and Land Development*, (51); 78–93

Byun, H. R. and D. A. Wilhite (1999). Objective Quantification of Drought Severity and Duration. *Journal of Climate*, **12**(9); 2747–2756

Chandrasekara, S. S., H.-H. Kwon, M. Vithanage, J. Obeysekera, and T. W. Kim (2021). Drought in South Asia: A Review of Drought Assessment and Prediction in South Asian Countries. *Atmosphere*, **12**(3); 369

Daoed, D., B. Rusman, B. Istijono, A. Hakam, and M. Syukur (2018). Evaluation of Drought Vulnerability on Watersheds in West Sumatera Province by using Cropwat-8 and GIS. *International Journal on Advanced Science, Engineering and Information Technology*, **8**(6); 2443–2449

Darlan, N. H., S. S. Arif, P. Sudira, and B. D. A. Nugroho (2020). Spatial and Temporal Analysis of Seasonal Rainfall on the East Coast of North Sumatra, Indonesia. *Indonesian Journal of Geography*, **52**(3); 360–367

Davies, S. J. and L. Unam (1999). Smoke-haze from the 1997 Indonesian Forest Fires: Effects on Pollution Levels, Local Climate, Atmospheric CO2 Concentrations, and Tree Photosynthesis. *Forest Ecology and Management*, **124**(2-3); 137–144

Edwards, D. C. and T. B. McKee (1997). *Characteristics of 20 th Century Drought in the United States at Multiple Time Scales*, volume 97. Colorado State University Fort Collins

Eslamian, S., K. Ostad Ali Askari, V. P. Singh, N. R. Dalezios, M. Ghane, Y. Yihdego, and M. Matouq (2017). A Review of Drought Indices. *International Journal of Constructive Research in Civil Engineering*, **3**; 48–66

Huang, Y. F., J. T. Ang, Y. J. Tiong, M. Mirzaei, and M. Z. M. Amin (2016). Drought Forecasting using SPI and EDI under RCP-8.5 Climate Change Scenarios for Langat River Basin, Malaysia. *Procedia Engineering*, **154**; 710–717

Iskandar, I., M. Irfan, F. Syamsuddin, A. Johan, and P. Poerwono (2011). Trend in Precipitation Over Sumatera Under the Warming Earth. *International Journal of Remote Sensing and Earth Sciences (IJReSES)*, **8**(1)

Iskandar, I., W. Mardiansyah, D. Setiabudidaya, P. Poerwono, I. Yusyian, and Z. Dahlan (2017a). What Did Drive Extreme Drought Event in Indonesia During Boreal Summer/fall 2014? *Journal of Physics: Conference Series*, **817**(1); 012073

Iskandar, I., P. A. Utari, D. O. Lestari, Q. W. Sari, D. Setiabudidaya, M. Khakim, I. Yustian, and Z. Dahlan (2017b). Evolution of 2015/2016 El Niño and its Impact on Indonesia. **1857**(1)

Jain, V. K., R. P. Pandey, M. K. Jain, and H. R. Byun (2015). Comparison of Drought Indices for Appraisal of Drought Characteristics in the Ken River Basin. *Weather and Climate Extremes*, **8**; 1–11

Kamruzzaman, M., S. Hwang, J. Cho, M. W. Jang, and H. Jeong (2019). Evaluating the Spatiotemporal Characteristics of Agricultural Drought in Bangladesh using Effective Drought Index. *Water*, **11**(12); 2437

Kurniadi, A., E. Weller, S. K. Min, and M. G. Seong (2021). Independent ENSO and IOD Impacts on Rainfall Extremes Over Indonesia. *International Journal of Climatology*, **41**(6); 3640–3656

Kuswanto, H., F. Hibatullah, and E. S. Soedjono (2019). Perception of Weather and Seasonal Drought Forecasts and its Impact on Livelihood in East Nusa Tenggara, Indonesia. *Heliyon*, *5*(8)

Lee, H. S. (2015). General Rainfall Patterns in Indonesia and the Potential Impacts of Local Seas On Rainfall Intensity. *Water*, **7**(4); 1751–1768

McKee, T. B., N. J. Doesken, and J. Kleist (1993). The Relationship of Drought Frequency and Duration to Time Scales. *Proceedings of Eighth Conference on Applied Climatology*, **17**(22); 179–183

Mori, S., H. Jun Ichi, Y. I. Tauhid, M. D. Yamanaka, N. Okamoto, F. Murata, N. Sakurai, H. Hashiguchi, and T. Sribimawati (2004). Diurnal Land–sea Rainfall Peak Migration Over Sumatera Island, Indonesian Maritime Continent, Observed by TRMM Satellite and Intensive Rawinsonde Soundings. *Monthly Weather Review*, **132**(8); 2021–2039

Nita, I., A. N. Putra, and A. Fibrianingtyas (2020). Analysis of Drought Hazards in Agricultural Land in Pacitan Regency, Indonesia. *SAINS TANAH-Journal of Soil Science and Agroclimatology*, **17**(1); 7–15

Nurdiati, S., F. Bukhari, M. T. Julianto, A. Sopaheluwakan, M. Aprilia, I. Fajar, P. Septiawan, and M. K. Najib (2022). The Impact of El Niño Southern Oscillation and Indian Ocean Dipole on the Burned Area in Indonesia. *Terrestrial, Atmospheric and Oceanic Sciences*, **33**(1); 16

Nurdiati, S., A. Sopaheluwakan, and P. Septiawan (2021). Spatial and Temporal Analysis of El Niño Impact on Land and Forest Fire in Kalimantan and Sumatra. *Agromet*, **35**(1); 1–10

Park, C. K., J. Kam, H. R. Byun, and D. W. Kim (2022). A self-calibrating Effective Drought Index (scEDI): Evaluation Against Social Drought Impact Records Over the Korean Peninsula (1777–2020). *Journal of Hydrology*, **613**; 128357

Pramudya, Y., T. Onishi, M. Senge, K. Hiramatsu, and P. M. Nur (2019). Evaluation of Recent Drought Conditions by Standardized Precipitation Index and Potential Evapotran-

spiration Over Indonesia. *Paddy and Water Environment*, **17**; 331–338

Prinz, D. (2009). Contributor and Victim-Indonesia's Role in Global Climate Change with Special Reference to Kalimantan. *Jurnal Sains & Teknologi Lingkungan*, **1**(2); 139–153

Qian, J. H. (2020). Multi-scale Climate Processes and Rainfall Variability in Sumatra and Malay Peninsula Associated with ENSO in Boreal Fall and Winter. *International Journal of Climatology*, **40**(9); 4171–4188

Raude, J. M., R. M. Wambua, and B. M. Mutua (2018). Detection of Spatial, Temporal and Trend of Meteorological Drought Using Standardized Precipitation Index (SPI) and Effective Drought Index (EDI) in the Upper Tana River Basin. *Open Journal of Modern Hydrology*, **8**; 83–100

Saji, N. and T. Yamagata (2003). Possible Impacts of Indian Ocean Dipole Mode Events on Global Climate. *Climate Research*, **25**(2); 151–169

Salehnia, N., A. Alizadeh, H. Sanaeinejad, M. Bannayan, A. Zarrin, and G. Hoogenboom (2017). Estimation of Meteorological Drought Indices based on AgMERRA Precipitation Data and Station-observed Precipitation Data. *Journal of Arid Land*, **9**; 797–809

Sarmiasih, M. and P. Y. Pratama (2019). The Problematics Mitigation of Forest and Land Fire District (Kerhutla) in Policy Perspective (A Case Study: Kalimantan and Sumatra in Period 2015-2019). *Journal of Governance and Public Policy*, **6**(3); 270–292

Supari, S., I. Iskandar, M. Irfan, and H. Akhsan (2023). Drought Assessment in Aceh and North Sumatra Using Effective Drought Index. *Science and Technology Indonesia*, **8**(2)

Supari, S., R. Muharsyah, and A. Sopaheluwakan (2016). Mapping Drought Risk in Indonesia Related to El-Niño Hazard. *AIP Conference Proceedings*, **1730**(1)

Svoboda, M. and B. Fuchs (2016). Handbook of Drought Indicators and Indices. *Drought and Water Crises: Integrating Science, Management, and Policy*; 155–208

WMO (2012). Standardized Precipitation Index User Guide. *World Meteorological Organization*, **1090**

WMO (2016). Handbook of Drought Indicators and Indices. *In British Medical Journal*; 2366

Zargar, A., R. Sadiq, B. Naser, and F. I. Khan (2011). A Review of Drought Indices. *Environmental Reviews*, **19**(NA); 333–349

